



Individual differences in GABA content are reliable but are not uniform across the human cortex



Ian Greenhouse^{a,*}, Sean Noah^a, Richard J. Maddock^b, Richard B. Ivry^a

^a University of California, Berkeley, Berkeley, CA, United States

^b University of California, Davis, Davis, CA, United States

ARTICLE INFO

Article history:

Received 23 February 2016

Revised 1 May 2016

Accepted 6 June 2016

Available online 09 June 2016

Keywords:

Individual differences

GABA

Magnetic resonance spectroscopy

Cortex

Molecular topography

Inhibition

ABSTRACT

¹H magnetic resonance spectroscopy (MRS) provides a powerful tool to measure gamma-aminobutyric acid (GABA), the principle inhibitory neurotransmitter in the human brain. We asked whether individual differences in MRS estimates of GABA are uniform across the cortex or vary between regions. In two sessions, resting GABA concentrations in the lateral prefrontal, sensorimotor, dorsal premotor, and occipital cortices were measured in twenty-eight healthy individuals. GABA estimates within each region were stable across weeks, with low coefficients of variation. Despite this stability, the GABA estimates were not correlated between regions. In contrast, the percentage of brain tissue per volume, a control measure, was correlated between the three anterior regions. These results provide an interesting dissociation between an anatomical measure of individual differences and a neurochemical measure. The different patterns of anatomy and GABA concentrations have implications for understanding regional variation in the molecular topography of the brain in health and disease.

© 2016 Elsevier Inc. All rights reserved.

Introduction

Immunohistochemical, enzymatic, chromatographic and radio-receptor assays in humans and non-human species have demonstrated that γ -aminobutyric acid (GABA) concentrations vary across brain regions (Baxter, 1970). The initial work on this problem, performed predominantly *ex vivo*, helped establish GABA's role as the primary inhibitory neurotransmitter in the vertebrate brain. Recent studies have focused on the local distribution of GABA receptor subtypes (Watanabe et al., 2002), including genetic contributions to the molecular topography across the entire brain (Hawrylycz et al., 2012). While this work has characterized synaptic GABA mechanisms and suggests that gene transcription is relatively homogenous throughout the neocortex, an open question concerns whether individual differences in GABA levels are uniform throughout the cortex or are region-specific. The answer to this question is important for understanding GABA's role in mediating widespread versus local brain functions.

In vivo ¹H magnetic resonance spectroscopy (MRS) measures metabolite concentrations, including GABA, with sufficient sensitivity to detect individual differences. To date, three studies have assayed different regions and reported that GABA levels were not correlated between brain regions (Boy et al., 2010; Grachev and Apkarian, 2000; Grachev et al., 2001). However, these studies did not assess measurement

reliability, a prerequisite for investigating individual differences. Consequently, the lack of relationships between brain regions in these studies could arise from inter-regional differences in measurement reliability.

To evaluate the spatial scale at which GABA levels are mediated in the brain, we obtained Mescher-Garwood point-resolved spectroscopy (MEGA-PRESS) measurements of GABA from the lateral prefrontal (LPF), sensorimotor (SM), dorsal premotor (PMd), and occipital (OCC) cortices. Measurements were made during two separate sessions, approximately two weeks apart, to assess reliability (Bogner et al., 2010; Evans et al., 2010; Geramita et al., 2011; Near et al., 2014; O'Gorman et al., 2011; Stephenson et al., 2011). These measurements were combined across the two sessions and used to compare GABA estimates between regions. As a point of contrast, we compared brain tissue per volume between the same four measurement regions. This measure and a coregistration procedure were used to assess the reliability of voxel positioning across sessions.

Materials and methods

Participants

Twenty-eight males (21.8 ± 0.4 years of age) were scanned in two sessions (16 ± 3 days apart). All participants provided informed consent following a protocol approved by the IRB of the University of California, Berkeley, and were screened for magnetic resonance imaging contraindications.

* Corresponding author at: 3201 Tolman Hall, University of California, Berkeley, Berkeley, CA 94720-1650, United States.

E-mail address: igreenhouse@berkeley.edu (I. Greenhouse).

Magnetic resonance imaging and spectroscopy acquisition

MR data were acquired using a 3 Tesla Siemens TIM/trio scanner (Berlin/Munich, Germany) with a 32-channel radiofrequency head coil. Each scanning session consisted of two T1-weighted anatomical scans (sagittal MPRAGE, TR/TE = 1900/2.52 ms, 900 ms TI, flip angle = 9°, FoV 250 × 176, 1 mm³ voxel size, acceleration factor of two) and eight MEGA-PRESS scans (320 transients per scan – 160 Off and 160 On, TR/TE = 1500/68 ms, 1.9 ppm and 7.5 ppm On- and Off-resonance edit pulse frequencies, 45 Hz edit pulse bandwidth, delta frequency of –1.7 ppm relative to water – optimized for signal detection at 3.00 ppm, 50 Hz water suppression bandwidth, TA = 8.4 min). MEGA-PRESS averages were collected in pairs, alternating between On- and Off-resonance editing pulses.

MRS data were acquired within each of four voxels, designed to target right lateral prefrontal cortex (LPF; 25 × 40 × 25 mm), right sensorimotor cortex (SM; 30 × 30 × 30 mm), right dorsal premotor cortex (PMd; 25 × 40 × 25 mm), and bilateral occipital cortex (OCC; 30 × 30 × 30 mm). Voxel orientations maximized the amount of grey matter relative to white matter and CSF within each voxel, while also accommodating each individual participant's anatomy. The LPF and SM voxels were prescribed in reference to the first T1-weighted scan, and the PMd and OCC voxels were prescribed in reference to the second T1-weighted scan. Thus, the imaging protocol consisted of one T1 weighted scan followed by LPF (×2) and SM (×2) acquisitions. A separate T1 weighted scan was then acquired, followed by PMd (×2) and OCC (×2, if time allowed) MRS acquisitions. Shimming for each voxel involved a

combined automated and manual routine that was performed immediately after each voxel was positioned. Each voxel was sampled in two consecutive 8.4-minute scans and the order of scans was consistent across all participants and visits. Maintaining a constant order for all participants controlled for temporal relationships that could influence data acquisition during each scan session.

The T1-weighted image was resliced into axial and coronal views, and voxels were positioned relative to anatomical landmarks using all three planar views (Fig. 1A). The outer surfaces of all voxels remained several millimeters inside the brain to allow for imperfect RF profiles for volume selection and editing, a limitation of the MEGA-PRESS sequence (Kaiser et al., 2008) and ensured that measurements did not extend outside the cortical surface. Gradient orders for each voxel were optimized to reduce artifacts as determined during pilot testing (Ernst and Chang, 1996).

The LPF voxel was centered over the inferior frontal junction, with the longest axis extending anterior to posterior. One surface of the LPF voxel followed the outer surface of the cortex in both the coronal and axial views. The SM voxel was centered over the hand knob, parallel to the anterior to posterior axis. One surface of the SM voxel was parallel to the cortical surface in the coronal and axial views. The PMd voxel was positioned with its posterior surface aligned to the precentral sulcus, the lateral surface parallel to the right medial wall of the longitudinal fissure, and the dorsal surface parallel to the cortical surface along the anterior to posterior axis. The OCC voxel was centered bilaterally over the calcarine sulcus extending equally into the left and right hemispheres. The ventral surface of the OCC voxel was parallel to the straight sinus.

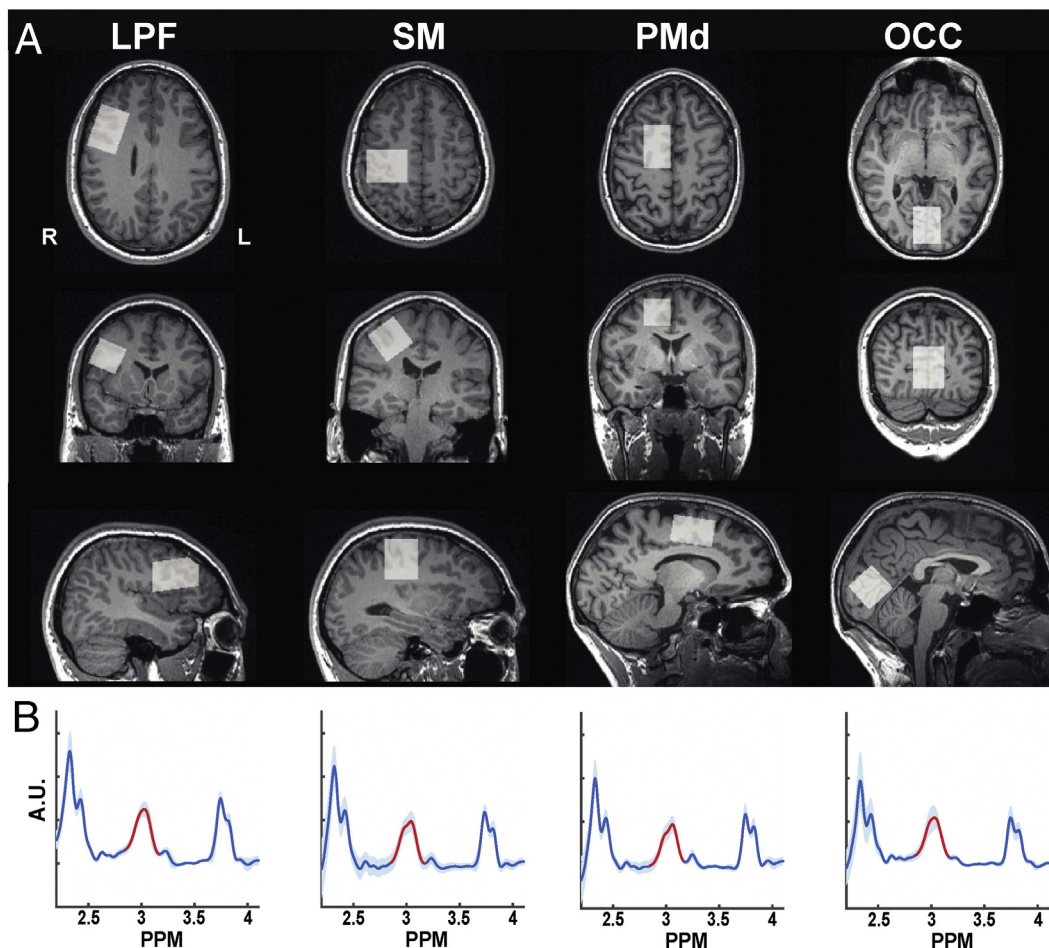


Fig. 1. Voxel positioning and GABA estimation. (A) MRS measurements were made during two scanning sessions from voxels prescribed in the lateral prefrontal (LPF), sensorimotor (SM), dorsal premotor (PMd), and occipital (OCC) cortices. (B) GABA+ signal was quantified by integrating the difference spectra under the peak centered at 3.00 ppm. Group means (solid lines) and standard deviations (shaded regions) are shown.

Sagittal, axial, and coronal views of each voxel, registered to the T1-weighted image acquired at the first session, were used to guide positioning of each voxel at the second session. First, the center coordinates and orientation for each voxel from the first session were used to initialize the position of each voxel at the second session. To adjust for differences in head position, manual translations and rotations were made using the anatomical landmarks identified during the first session.

Data analysis

All data were analyzed using customized routines in Matlab (Natick, MA). The scans were exported in Siemens .rda format, with sets of 10 consecutive transients averaged and stored in a single .rda file. This yielded 32 .rda files for each scan (16 On and 16 Off). Preprocessing of the spectra included zero-filling spectra from 1024 to 4096 data points and apodization with a 4 Hz Gaussian function. Off-resonance spectra were manually phase corrected and aligned with reference to creatine (Cr). Correction values were applied to the paired On-resonance spectra (Evans et al., 2013; Near et al., 2015). The mean and standard deviation were calculated at each frequency of each On- and Off-resonance spectrum, and the number of deviant values (>2 standard deviations from the mean) was tallied. The spectra were visually inspected to identify those which should be excluded from further analysis based on the number of deviant values and overt corruption or distortion of the spectra (Near et al., 2013; Simpson et al., 2015). The complete analysis code is available for download at <https://osf.io/3gsdt/>. The mean number of spectra removed was $0.5 \pm 0.4\%$ for the LPF, $0.4 \pm 0.3\%$ for the SM, $0.3 \pm 0.2\%$ for the PMd, and 0% for the OCC voxel. There was no evidence that the quality of data changed within a session or between sessions as assessed by the number of deviant values.

Peak integration was performed using a previously published method (Yoon et al., 2010; Maddock et al., 2016). In brief, the signal was integrated beneath the GABA+ peak (range: 2.85 to 3.15 ppm, Fig. 1B) in the difference spectra and the Cr peak (range: 2.93 to 3.10 ppm) in the summed On- and Off-resonance spectra. The ratio of total GABA+ to total Cr signal (GABA+/Cr) was calculated from the average preprocessed spectra acquired within each scan. This GABA+/Cr ratio accounts for scanner-related factors that might impact signal-to-noise differently within/between scans or days, and that could differentially impact reference peaks away from 3 ppm (Mullins et al., 2014). Data included in the final analyses were comprised of spectra from two scans (160 measures each) acquired within each session (4 total scans) and screened for artifacts. Participants who provided three or fewer scans were excluded. This conservative approach to data inclusion yielded LPF data from 20 participants, SM data from 22 participants, PMd data from 24 participants, and OCC data from 15 participants. Due to time constraints in the scanner, and because the OCC voxel was always acquired last, the OCC data were only acquired in a subset of participants at both sessions. We note that the OCC findings are considered exploratory because they were obtained from a smaller sample.

Pearson correlations of GABA+/Cr ratios between sessions were performed to assess reliability across days for each voxel, and coefficients of variation were calculated within participants for each voxel, as an estimate of the signal-to-noise ratio. Using the data averaged across the two sessions, Pearson correlations between pairs of voxels were performed to test whether individual differences in GABA+/Cr ratios in one brain area predicted differences in another brain area. The same comparisons were performed for GABA+ estimates alone to rule out the possibility that Cr estimates might account for any observed relationships. The GABA+ estimates taken on their own are more susceptible to differences in the magnetic field across scans or other scanner related factors, but this analysis helps to constrain interpretations.

The percent total volume of grey matter, white matter, and cerebrospinal fluid (CSF) were calculated within each voxel using the FMRIB's

Automated Segmentation Tool (Zhang et al., 2001; <http://fsl.fmrib.ox.ac.uk/>). The percent tissue relative to total voxel volume ([grey matter + white matter] / total volume) was first used to compare the reliability of voxel placement between the two scans. Agreement between scans is unlikely to be accounted for by artifacts that are specific to a single scan, such as head motion. These same measures were used to compare percent tissue between voxels. We note that while head motion might globally affect T1-weighted images, we used one T1-weighted image to calculate tissue percentages for the PMd and OCC voxels and a separate T1-weighted image to calculate tissue percentages for the LPF and SM voxels at each session. This approach controlled for motion artifacts that could introduce artificial relationships in tissue estimates across regions that would be expected for an image derived from a single scan.

To further assess the reliability of voxel placement between visits, we coregistered the T1-weighted images from the second visit to those acquired at the first visit using the FMRIB FLIRT registration toolbox (rigid-body coregistration with six degrees of freedom). The resulting registration matrices were applied to three-dimensional reconstructed masks of the MRS voxels acquired at the second visit, with reference to the appropriate T1-weighted images. After coregistration, we calculated the percent overlap of each pair of voxels between visits (e.g., the LPF voxel at visit 1 relative to the LPF voxel at visit 2) using the `fslmaths` tools.

Total tissue percentage, percent GM, and percent WM for each voxel were correlated with the metabolite estimates to test for relationships between GABA+/Cr and tissue subtypes. Coefficients of variation (CVs) were used to assess the relative variability of measurements across sessions, with lower values reflecting greater reliability.

Results

Percent brain tissue is reliable but not correlated with GABA+/Cr ratios

Tissue percentages within each voxel were highly correlated across sessions (LPF: $r = 0.82$, $p < 0.001$, SM: $r = 0.89$, $p < 0.001$, PMd: $r = 0.82$, $p < 0.001$, OCC: $r = 0.82$, $p < 0.001$; Fig. 2A) and exhibited low CVs (Table S1). A similar pattern was observed for percent GM and percent WM (Figs. S1 & S2, & Table S1). Averaged across sessions, percent total tissue was $91 \pm 0.03\%$, $90 \pm 0.04\%$, $91 \pm 0.03\%$, and $90 \pm 0.04\%$ for the LPF, SM, PMd, and OCC voxels, respectively. The coregistration procedure showed that there was $90.6 \pm 1.4\%$ overlap between sessions for the LPF voxels, $90.5 \pm 1.9\%$ overlap for the SM voxel, $90.9 \pm 2.0\%$ overlap for the PMd voxel, and $89.8 \pm 2.5\%$ overlap for the OCC voxel. We note that the automated coregistration method may introduce some error.

GABA+/Cr ratios were not correlated with tissue percentages (Fig. 2B), percent GM (Fig. S3), or percent WM (Fig. S4) within any voxel. For this reason, and because we did not estimate absolute concentrations (Kreis et al., 1993a, 1993b), we did not “correct” our GABA+/Cr estimates as a function of tissue volume estimates, e.g. (Harris et al., 2015). Furthermore, we did not observe any relationships between tissue composition and GABA+ or Cr estimates alone for any of our voxels (GM and GABA+: all voxels $p > 0.13$, Fig. S5; WM and GABA+: all voxels $p > 0.14$, Fig. S6; GM and Cr: all voxels $p > 0.27$, Fig. S7; WM and Cr: all voxels $p > 0.11$, Fig. S8).

GABA+/Cr ratios and GABA+ alone are reliable within sessions and across weeks

The GABA+/Cr ratios were reliable between the two scans within each session (LPF: $R = 0.75$, $p < 0.001$, $CV = 4.6 \pm 0.9\%$; SM: $R = 0.64$, $p < 0.01$, $CV = 3.9 \pm 1.0\%$; PMd: $R = 0.63$, $p < 0.005$, $CV = 3.9 \pm 0.7\%$; OCC: $R = 0.52$, $p < 0.05$, $CV = 5.3 \pm 1.1\%$). GABA+/Cr ratios were also stable across weeks in all four voxels (Fig. 3A). The CVs were $5.9 \pm 0.93\%$ (range 0.7–16.1%) for LPF, $5.3 \pm 0.98\%$ (range 0.2–16.9%)

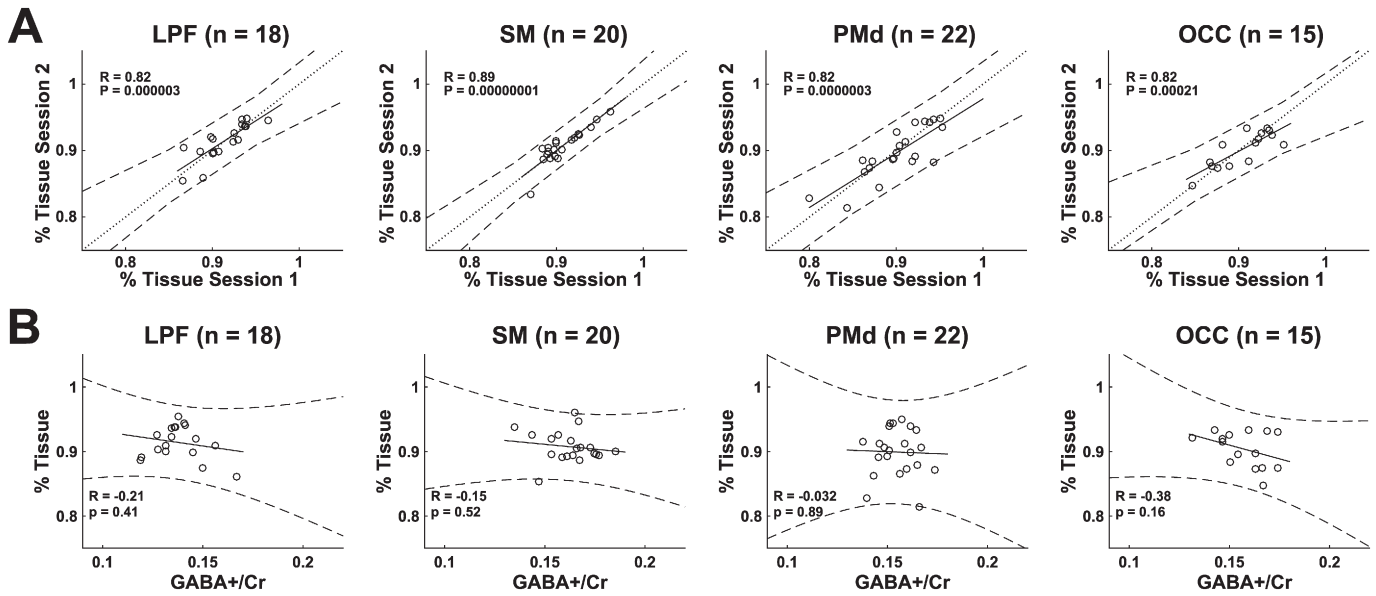


Fig. 2. Reliability of voxel positioning and percent tissue correlation with GABA +/Cr. (A) Tissue density within the lateral prefrontal (LPF), sensorimotor (SM), dorsal premotor (PMd), and occipital (OCC) voxels were highly reliable across sessions in all four voxels. (B) Using average measures across sessions, percent tissue per volume did not predict GABA +/Cr ratios.

for SM, $3.8 \pm 0.60\%$ (range 0.04–11.6%) for PMd, and $5.3 \pm 0.92\%$ (range 0.73–16.0%) for OCC voxels. These values are in agreement with previous studies (Evans et al., 2010; Near et al., 2014; Stephenson et al., 2011; Wijtenburg et al., 2013). Estimates of GABA + alone, expressed in arbitrary units, exhibited a similar pattern of reliability, although the correlation in OCC only reached trend-level significance (LPF: $r = 0.46$, $p < 0.05$, SM: $r = 0.7$, $p < 0.001$, PMd: $r = 0.56$, $p < 0.005$, OCC: $r = 0.49$, $p = 0.06$; Fig. 3B).

GABA +/Cr and tissue comparisons across brain regions

The preceding analyses indicate that MR scanner performance and MRS voxel positioning were consistent across the two sessions. Moreover, the observed reliability for the GABA +/Cr ratios cannot be explained by Cr measurements alone. This allowed us to turn to our

main question: whether individual differences in intrinsic GABA are consistent between cortical regions.

We averaged the GABA +/Cr ratios across the two sessions and tested for correlations between each pair of voxels. Importantly, individual differences in GABA +/Cr within one voxel did not predict individual differences at the other voxels (all p 's > 0.06 , Fig. 4A). This result suggests that intrinsic cortical GABA + content is determined locally. The correlation approached significance for the PMd and SM voxels ($p = 0.06$), although it is important to keep in mind that, because of their proximity, these two voxels overlapped by approximately 5% of their total volume ($11.2 \pm 5.3 \text{ mm}^3$).

In contrast to GABA +/Cr, total tissue percentages were correlated between the LPF, SM, and PMd voxels (all p 's < 0.05 uncorrected, Fig. 4B), with only the correlation between the SM and PMd voxels surviving a more stringent multiple comparison correction ($p < 0.0125$).

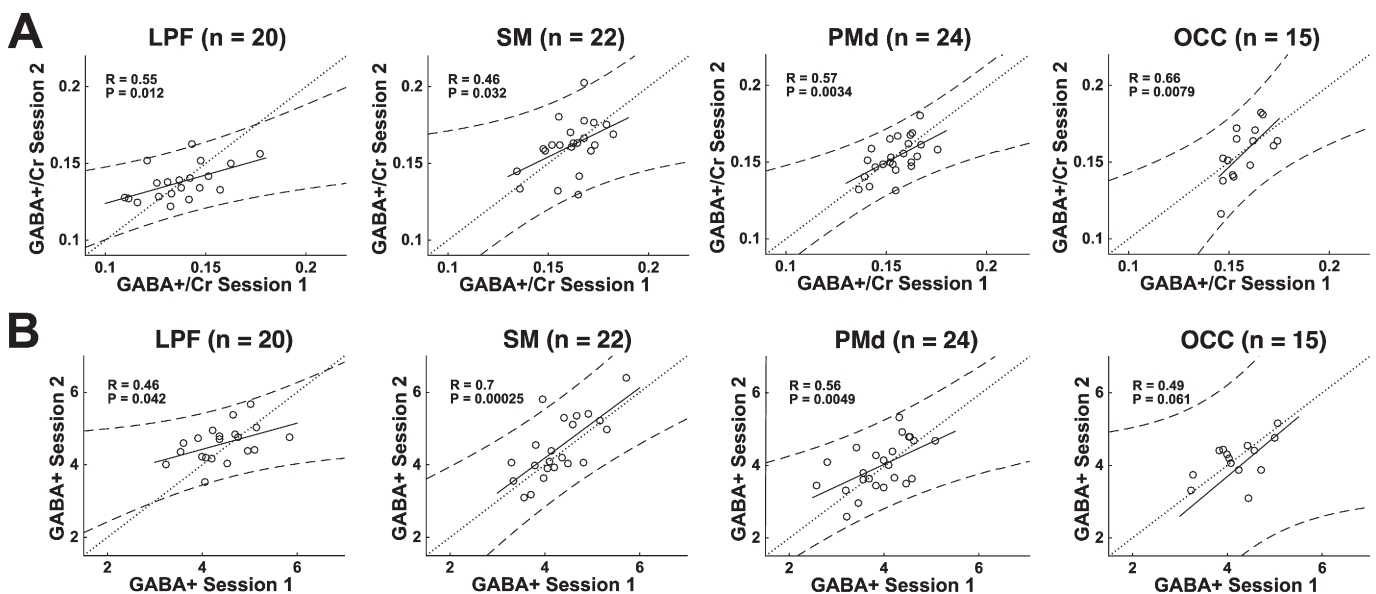


Fig. 3. GABA +/Cr ratios and raw GABA + estimates were reliable. (A) GABA +/Cr ratios were reliable across sessions within the lateral prefrontal (LPF), sensorimotor (SM), dorsal premotor (PMd), and occipital (OCC) voxels. (B) GABA + estimates were also reliable across sessions, indicating that scanning related factors were consistent between days and that Cr alone is unlikely to account for the reliable GABA +/Cr ratios.

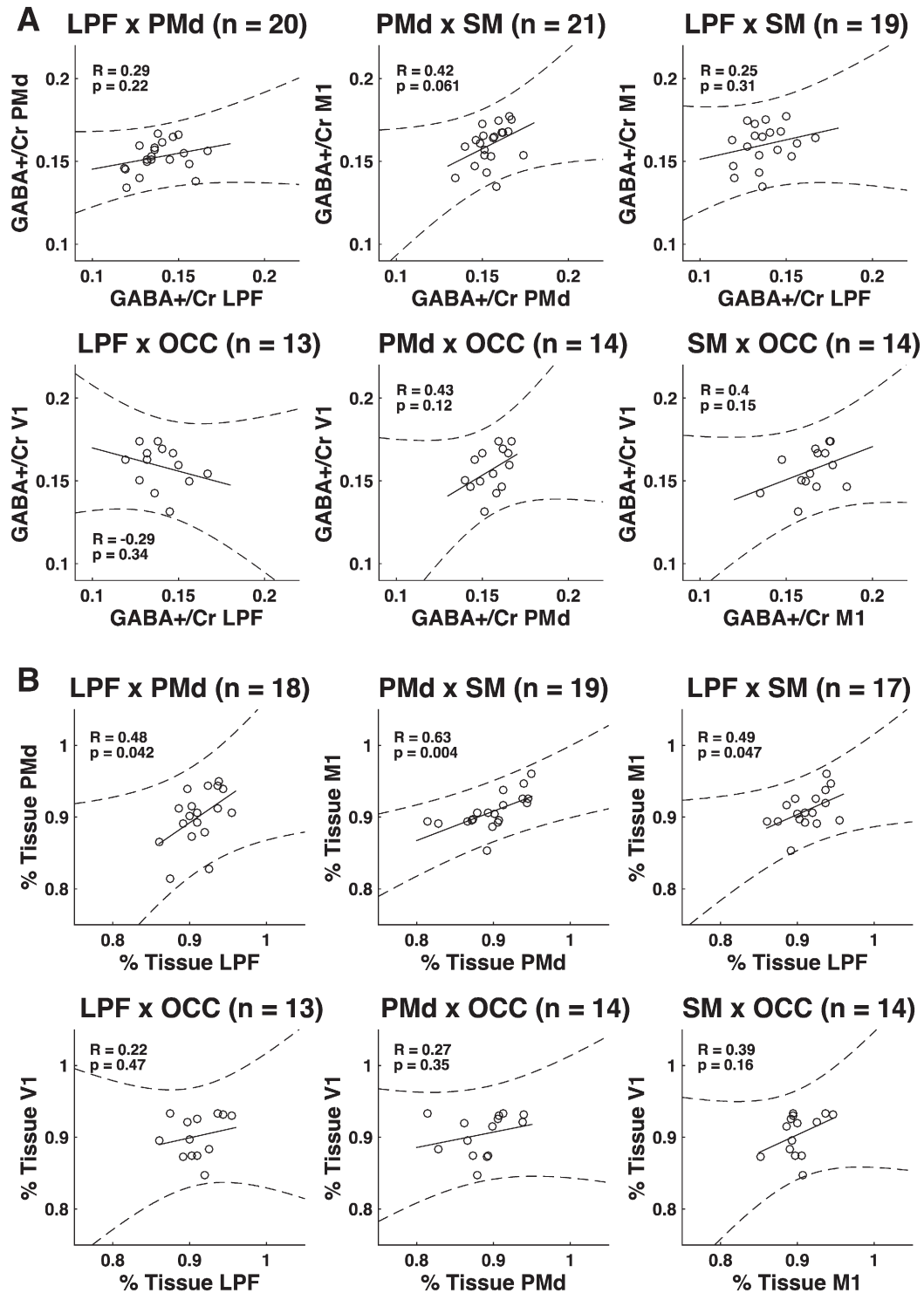


Fig. 4. Tissue density but not GABA +/Cr is correlated between voxels. (A) GABA +/Cr ratios were not significantly correlated in any pairwise comparison of the four voxels. (B) Tissue density was correlated between the lateral prefrontal (LPF), sensorimotor (SM), and dorsal premotor (PMd) voxels, but these frontal regions were not correlated with the occipital (OCC) voxel.

Thus, individual differences in total tissue percentages were consistent between the anterior voxels.

Discussion

The study of individual differences is essential for understanding behavioral and biological variation. In the neurosciences, this approach lends insight into biomarkers of brain function and gene-

environment interactions. A recurring question concerns the regional specificity versus uniformity of individual differences throughout the brain. For example, recent evidence suggests that a relatively homogenous ‘transcriptional blueprint’ exists throughout the cortex (Hawrylycz et al., 2012; Richiardi et al., 2015). Epigenetic factors demonstrate homogeneity across brain regions as well. Specifically, DNA methylation is more similar across different brain regions within an individual than for a single brain region compared across

individuals (Illingworth et al., 2015). Moreover, individual differences in white matter integrity (Penke et al., 2010) and diffusivity (Johnson et al., 2015), as well as grey matter density (Mechelli et al., 2005), are relatively uniform throughout the brain. All of these general factors could influence neurotransmitter concentrations. Indeed, local tissue percentages and tissue types have previously been linked to brain metabolite concentrations, including GABA (Bergmann et al., 2015; Harris et al., 2015; Jensen et al., 2005; Kreis et al., 1993b, 1993a).

Given these considerations it is surprising that individual differences in GABA +/Cr ratios were not correlated between neighboring cortical regions. These results are consistent with previous assessments of regional variation in GABA (Boy et al., 2010; Grachev and Apkarian, 2000) and provide two important advances. First, we performed comparisons between regions after establishing measurement reliability across two sessions, a prerequisite for studying individual differences. Notably, intra-voxel reliability was assessed between sessions, whereas comparisons between regions included data acquired within sessions. Our conclusions are thus conservative in that inter-session variability should impact reliability estimates to a greater degree than between-region comparisons. Second, the local variation in intrinsic GABA stands in contrast to a structural measure: The percentage of brain tissue, within the same voxels, was correlated between anterior cortical regions. Taken together, these measures suggest that anatomical and neurochemical individual differences occur at different spatial scales in the cortex.

Previous MRS studies reported correlations between behavioral or neurophysiological measures and GABA estimates within targeted brain regions (Bachtiar et al., 2015; Balz et al., 2016; Boy et al., 2010; Heba et al., 2016; Jocham et al., 2012; Stagg et al., 2011a, 2011b; Sumner et al., 2010; van Loon et al., 2013). For example, resting GABA content in primary motor cortex was positively correlated with individual differences in motor sequence reaction time (Stagg et al., 2011a). Our results are consistent with the hypothesis that locally determined neurotransmitter content relates to the functional specialization of brain regions. Moreover, the finding that resting GABA measurements within multiple cortical regions remained relatively stable across weeks suggests that task-dependent changes in GABA (Floyer-Lea et al., 2006; Michels et al., 2012) likely occur on top of stable basal levels.

Our results have important clinical implications. Abnormalities in GABA concentrations have been associated with neurological diseases and trauma (Blicher et al., 2015; Dharmadhikari et al., 2015; Draper et al., 2014; Hattingen et al., 2014; van der Hel et al., 2013). Given the reliability observed here in healthy individuals, it may be possible to relate local changes in GABA to patterns of recovery. Similarly, one could assess the anatomical specificity of medications that impact GABA-dependent processes, e.g. benzodiazepines or selective serotonin reuptake inhibitors (Bhagwagar et al., 2004).

The MRS method applied here measures metabolite concentrations throughout the entire voxel, including perivesicular and cytoplasmic environments. While we did not observe inter-regional correlations in GABA measurements, it is possible that specific compartments, e.g. vesicular or synaptic GABA, are similar across brain regions. Furthermore, we only studied young adult males. Our results may not translate to females or to older populations, as GABA content has been found to differ between the sexes (Epperson et al., 2002; O'Gorman et al., 2011) and to decrease with age (Gao et al., 2013). In addition, the GABA + signal at 3.00 ppm includes contributions from coedited macromolecules as well as homocarnosine, a GABA derivative; indeed, this is a principle limitation of the method. We did not control for macromolecules in our data, and the effects we observed could include a macromolecular contribution. It is also possible that differences in creatine content between regions influenced our results.

In summary, measurements of GABA +/Cr obtained across weeks exhibited marked reliability, but had little shared variance across brain

regions. Thus, while individual differences in cortical GABA concentrations are stable, variation in these concentrations is locally determined. These results support the use of MRS for assessing local neurotransmitter concentrations, with potential clinical utility for assessing sensitivity to treatment interventions or monitoring disease progression.

Acknowledgements

This work was supported by NIH grant NS085570. We thank Jamie Near for sharing analysis code and Ben Inglis and Eunice Yang for constructive input on data collection and analysis.

Appendix A. Supplementary data

Supplementary data to this article can be found online at <http://dx.doi.org/10.1016/j.neuroimage.2016.06.007>.

References

- Bachtiar, V., Near, J., Johansen-Berg, H., Stagg, C.J., 2015. Modulation of GABA and resting state functional connectivity by transcranial direct current stimulation. *Elife* 4, 1023. <http://dx.doi.org/10.7554/eLife.08789>.
- Balz, J., Keil, J., Roa Romero, Y., Meke, R., Schubert, F., Aydin, S., Ittermann, B., Gallinat, J., Senkowski, D., 2016. GABA concentration in superior temporal sulcus predicts gamma power and perception in the sound-induced flash illusion. *NeuroImage* 125, 724–730. <http://dx.doi.org/10.1016/j.neuroimage.2015.10.087>.
- Baxter, C.F., 1970. The nature of γ -aminobutyric acid. *Metabolic Reactions in the Nervous System*. Springer US, Boston, MA, pp. 289–353. http://dx.doi.org/10.1007/978-1-4615-7160-5_9.
- Bergmann, J., Pilatus, U., Genç, E., Kohler, A., Singer, W., Pearson, J., 2015. V1 surface size predicts GABA concentration in medial occipital cortex. *NeuroImage* 124, 654–662. <http://dx.doi.org/10.1016/j.neuroimage.2015.09.036>.
- Bhagwagar, Z., Wylezinska, M., Taylor, M., Jezzard, P., Matthews, P.M., Cowen, P.J., 2004. Increased brain GABA concentrations following acute administration of a selective serotonin reuptake inhibitor. *Am. J. Psychiatry* 161, 368–370. <http://dx.doi.org/10.1176/appi.ajp.161.2.368>.
- Blicher, J.U., Near, J., Naess-Schmidt, E., Stagg, C.J., Johansen-Berg, H., Nielsen, J.F., Østergaard, L., Ho, Y.-C.L., 2015. GABA levels are decreased after stroke and GABA changes during rehabilitation correlate with motor improvement. *Neurorehabil. Neural Repair* 29, 278–286. <http://dx.doi.org/10.1177/1545968314543652>.
- Bogner, W., Gruber, S., Doelken, M., Stadlbauer, A., Ganslandt, O., Boettcher, U., Trattng, S., Doerfler, A., Stefan, H., Hammen, T., 2010. In vivo quantification of intracerebral GABA by single-voxel (1)H-MRS-how reproducible are the results? *Eur. J. Radiol.* 73, 526–531. <http://dx.doi.org/10.1016/j.ejrad.2009.01.014>.
- Boy, F., Evans, C.J., Edden, R.A.E., Singh, K.D., Husain, M., Sumner, P., 2010. Individual differences in subconscious motor control predicted by GABA concentration in SMA. *Curr. Biol.* 20, 1779–1785. <http://dx.doi.org/10.1016/j.cub.2010.09.003>.
- Dharmadhikari, S., Ma, R., Yeh, C.-L., Stock, A.-K., Snyder, S., Zauber, S.E., Dydak, U., Beste, C., 2015. Striatal and thalamic GABA level concentrations play differential roles for the modulation of response selection processes by proprioceptive information. *NeuroImage* 120, 36–42. <http://dx.doi.org/10.1016/j.neuroimage.2015.06.066>.
- Draper, A., Stephenson, M.C., Jackson, G.M., Pèpès, S., Morgan, P.S., Morris, P.G., Jackson, S.R., 2014. Increased GABA contributes to enhanced control over motor excitability in Tourette syndrome. *Curr. Biol.* 24, 2343–2347. <http://dx.doi.org/10.1016/j.cub.2014.08.038>.
- Epperson, C.N., Haga, K., Mason, G.F., Sellers, E., Gueorguieva, R., Zhang, W., Weiss, E., Rothman, D.L., Krystal, J.H., 2002. Cortical gamma-aminobutyric acid levels across the menstrual cycle in healthy women and those with premenstrual dysphoric disorder: a proton magnetic resonance spectroscopy study. *Arch. Gen. Psychiatry* 59, 851–858.
- Ernst, T., Chang, L., 1996. Elimination of artifacts in short echo time H MR spectroscopy of the frontal lobe. *Magn. Reson. Med.* 36, 462–468.
- Evans, C.J., McGonigle, D.J., Edden, R.A.E., 2010. Diurnal stability of gamma-aminobutyric acid concentration in visual and sensorimotor cortex. *J. Magn. Reson. Imaging* 31, 204–209. <http://dx.doi.org/10.1002/jmri.21996>.
- Evans, C.J., Puts, N.A.J., Robson, S.E., Boy, F., McGonigle, D.J., Sumner, P., Singh, K.D., Edden, R.A.E., 2013. Subtraction artifacts and frequency (mis-)alignment in J-difference GABA editing. *J. Magn. Reson. Imaging* 38, 970–975. <http://dx.doi.org/10.1002/jmri.23923>.
- Floyer-Lea, A., Wylezinska, M., Kincses, T., Matthews, P.M., 2006. Rapid modulation of GABA concentration in human sensorimotor cortex during motor learning. *J. Neurophysiol.* 95, 1639–1644. <http://dx.doi.org/10.1152/jn.00346.2005>.
- Gao, F., Edden, R.A.E., Li, M., Puts, N.A.J., Wang, G., Liu, C., Zhao, B., Wang, H., Bai, X., Zhao, C., Wang, X., Barker, P.B., 2013. Edited magnetic resonance spectroscopy detects an age-related decline in brain GABA levels. *NeuroImage* 78, 75–82. <http://dx.doi.org/10.1016/j.neuroimage.2013.04.012>.
- Geramita, M., van der Veen, J.W., Barnett, A.S., Savostyanova, A.A., Shen, J., Weinberger, D.R., Marenco, S., 2011. Reproducibility of prefrontal γ -aminobutyric acid measurements with J-edited spectroscopy. *NMR Biomed.* 24, 1089–1098. <http://dx.doi.org/10.1002/nbm.1662>.

- Grachev, I.D., Apkarian, A.V., 2000. Chemical heterogeneity of the living human brain: a proton MR spectroscopy study on the effects of sex, age, and brain region. *NeuroImage* 11, 554–563. <http://dx.doi.org/10.1006/nimg.2000.0557>.
- Grachev, I.D., Swarnkar, A., Szevenenyi, N.M., Ramachandran, T.S., Apkarian, A.V., 2001. Aging alters the multichemical networking profile of the human brain: an in vivo (1)H-MRS study of young versus middle-aged subjects. *J. Neurochem.* 77, 292–303.
- Harris, A.D., Puts, N.A.J., Edden, R.A.E., 2015. Tissue correction for GABA-edited MRS: considerations of voxel composition, tissue segmentation, and tissue relaxations. *J. Magn. Reson. Imaging* 42, 1431–1440. <http://dx.doi.org/10.1002/jmri.24903>.
- Hattingen, E., Lücknerath, C., Pellikan, S., Vronski, D., Roth, C., Knake, S., Kieslich, M., Pilatus, U., 2014. Frontal and thalamic changes of GABA concentration indicate dysfunction of thalamofrontal networks in juvenile myoclonic epilepsy. *Epilepsia* 55, 1030–1037. <http://dx.doi.org/10.1111/epi.12656>.
- Hawrylycz, M.J., Lein, E.S., Guillozet-Bongaarts, A.L., Shen, E.H., Ng, L., Miller, J.A., van de Lagemaat, L.N., Smith, K.A., Ebbert, A., Riley, Z.L., Abajian, C., Beckmann, C.F., Bernard, A., Bertagnoli, D., Boe, A.F., Cartagena, P.M., Chakravarty, M.M., Chapin, M., Chong, J., Dalley, R.A., Daly, B.D., Dang, C., Datta, S., Dee, N., Dolbeare, T.A., Faber, V., Feng, D., Fowler, D.R., Goldy, J., Gregor, B.W., Haradon, Z., Haynor, D.R., Hohmann, J.G., Horvath, S., Howard, R.E., Jeromin, A., Jochim, J.M., Kinnunen, M., Lau, C., Lazarz, E.T., Lee, C., Lemon, T.A., Li, L., Li, Y., Morris, J.A., Overly, C.C., Parker, P.D., Parry, S.E., Reding, M., Royall, J.J., Schulkin, J., Sequeira, P.A., Slaughterbeck, C.R., Smith, S.C., Sott, A.J., Sunkin, S.M., Swanson, B.E., Vawter, M.P., Williams, D., Wohnoutka, P., Zielke, H.R., Geschwind, D.H., Hof, P.R., Smith, S.M., Koch, C., Grant, S.G.N., Jones, A.R., 2012. An anatomically comprehensive atlas of the adult human brain transcriptome. *Nature* 489, 391–399. <http://dx.doi.org/10.1038/nature11405>.
- Heba, S., Puts, N.A.J., Kalisch, T., Glaubitz, B., Haag, L.M., Lenz, M., Dinse, H.R., Edden, R.A.E., Tegenthoff, M., Schmidt-Wilcke, T., 2016. Local GABA concentration predicts perceptual improvements after repetitive sensory stimulation in humans. *Cereb. Cortex* 26, 1295–1301. <http://dx.doi.org/10.1093/cercor/bhv296>.
- Illingworth, R.S., Gruenewald-Schneider, U., De Sousa, D., Webb, S., Merusi, C., Kerr, A.R.W., James, K.D., Smith, C., Walker, R., Andrews, R., Bird, A.P., 2015. Inter-individual variability contrasts with regional homogeneity in the human brain DNA methylome. *Nucleic Acids Res.* 43, 732–744. <http://dx.doi.org/10.1093/nar/gku1305>.
- Jensen, J.E., deB Frederick, B., Renshaw, P.F., 2005. Grey and white matter GABA level differences in the human brain using two-dimensional, J-resolved spectroscopic imaging. *NMR Biomed.* 18, 570–576. <http://dx.doi.org/10.1002/nbm.994>.
- Jocham, G., Hunt, L.T., Near, J., Behrens, T.E.J., 2012. A mechanism for value-guided choice based on the excitation-inhibition balance in prefrontal cortex. *Nat. Neurosci.* 15, 960–961. <http://dx.doi.org/10.1038/nn.3140>.
- Johnson, M.A., Diaz, M.T., Madden, D.J., 2015. Global versus tract-specific components of cerebral white matter integrity: relation to adult age and perceptual-motor speed. *Brain Struct. Funct.* 220, 2705–2720. <http://dx.doi.org/10.1007/s00429-014-0822-9>.
- Kaiser, L.G., Young, K., Meyerhoff, D.J., Mueller, S.G., Matson, G.B., 2008. A detailed analysis of localized J-difference GABA editing: theoretical and experimental study at 4 T. *NMR Biomed.* 21, 22–32. <http://dx.doi.org/10.1002/nbm.1150>.
- Kreis, R., Ernst, T., Ross, B.D., 1993a. Development of the human brain: in vivo quantification of metabolite and water content with proton magnetic resonance spectroscopy. *Magn. Reson. Med.* 30, 424–437.
- Kreis, R., Ernst, T., Ross, B.D., 1993b. Absolute quantitation of water and metabolites in the human brain. II. Metabolite concentrations. *J. Magn. Reson. Ser. B* 102, 9–19. <http://dx.doi.org/10.1006/jmrb.1993.1056>.
- Maddock, R.J., Casazza, G.A., Fernandez, D.H., Maddock, M.L., 2016. Acute Modulation of Cortical Glutamate and GABA Content by Physical Activity. *J. Neurosci.* 36 (8), 2449–2457. <http://dx.doi.org/10.1523/JNEUROSCI.3455-15.2016>.
- Mechelli, A., Friston, K.J., Frackowiak, R.S., Price, C.J., 2005. Structural covariance in the human cortex. *J. Neurosci.* 25, 8303–8310. <http://dx.doi.org/10.1523/JNEUROSCI.0357-05.2005>.
- Michels, L., Martin, E., Klaver, P., Edden, R., Zelaya, F., Lythgoe, D.J., Luchinger, R., Brandeis, D., O’Gorman, R.L., 2012. Frontal GABA levels change during working memory. *PLoS One* 7, e31933. <http://dx.doi.org/10.1371/journal.pone.0031933>.
- Mullins, P.G., McGonigle, D.J., O’Gorman, R.L., Puts, N.A.J., Vidyasagar, R., Evans, C.J., Cardiff Symposium on MRS of GABA, Edden, R.A.E., 2014. Current practice in the use of MEGA-PRESS spectroscopy for the detection of GABA. *NeuroImage* 86, 43–52. <http://dx.doi.org/10.1016/j.neuroimage.2012.12.004>.
- Near, J., Evans, C.J., Puts, N.A.J., Barker, P.B., Edden, R.A.E., 2013. J-difference editing of gamma-aminobutyric acid (GABA): simulated and experimental multiplet patterns. *Magn. Reson. Med.* 70, 1183–1191. <http://dx.doi.org/10.1002/mrm.24572>.
- Near, J., Ho, Y.-C.L., Sandberg, K., Kumaragamage, C., Blicher, J.U., 2014. Long-term reproducibility of GABA magnetic resonance spectroscopy. *NeuroImage* 99, 191–196. <http://dx.doi.org/10.1016/j.neuroimage.2014.05.059>.
- Near, J., Edden, R., Evans, C.J., Paquin, R., Harris, A., Jezzard, P., 2015. Frequency and phase drift correction of magnetic resonance spectroscopy data by spectral registration in the time domain. *Magn. Reson. Med.* 73, 44–50. <http://dx.doi.org/10.1002/mrm.25094>.
- O’Gorman, R.L., Michels, L., Edden, R.A., Murdoch, J.B., Martin, E., 2011. In vivo detection of GABA and glutamate with MEGA-PRESS: reproducibility and gender effects. *J. Magn. Reson. Imaging* 33, 1262–1267. <http://dx.doi.org/10.1002/jmri.22520>.
- Penke, L., Maniega, S.M., Murray, C., Gow, A.J., Hernández, M.C.V., Clayden, J.D., Starr, J.M., Wardlaw, J.M., Bastin, M.E., Deary, I.J., 2010. A general factor of brain white matter integrity predicts information processing speed in healthy older people. *J. Neurosci.* 30, 7569–7574. <http://dx.doi.org/10.1523/JNEUROSCI.1553-10.2010>.
- Richiardi, J., Altmann, A., Milazzo, A.-C., Chang, C., Chakravarty, M.M., Banaschewski, T., Barker, G.J., Bokde, A.L.W., Bromberg, U., Büchel, C., Conrod, P., Fauth-Bühler, M., Flor, H., Frouin, V., Gallinat, J., Garavan, H., Gowland, P., Heinz, A., Lemaître, H., Mann, K.F., Martinot, J.-L., Nees, F., Paus, T., Pausova, Z., Rietschel, M., Robbins, T.W., Smolka, M.N., Spanagel, R., Ströhle, A., Schumann, G., Hawrylycz, M., Poline, J.-B., Greicius, M.D., IMAGEN consortium, 2015. BRAIN NETWORKS. Correlated gene expression supports synchronous activity in brain networks. *Science* 348, 1241–1244. <http://dx.doi.org/10.1126/science.1255905>.
- Simpson, R., Devenyi, G.A., Jezzard, P., Hennessy, T.J., Near, J., 2015. Advanced processing and simulation of MRS data using the FID appliance (FID-A)—an open source, MATLAB-based toolkit. *Magn. Reson. Med.* <http://dx.doi.org/10.1002/mrm.26091>.
- Stagg, C.J., Bachtir, V., Johansen-Berg, H., 2011a. The role of GABA in human motor learning. *Curr. Biol.* 21, 480–484. <http://dx.doi.org/10.1016/j.cub.2011.01.069>.
- Stagg, C.J., Bestmann, S., Constantinescu, A.O., Moreno, L.M., Allman, C., Mekte, R., Woolrich, M., Near, J., Johansen-Berg, H., Rothwell, J.C., 2011b. Relationship between physiological measures of excitability and levels of glutamate and GABA in the human motor cortex. *J. Physiol.* 589, 5845–5855. <http://dx.doi.org/10.1111/jphysiol.2011.216978>.
- Stephenson, M.C., Gunner, F., Napolitano, A., Greenhaff, P.L., Macdonald, I.A., Saeed, N., Vennart, W., Francis, S.T., Morris, P.G., 2011. Applications of multi-nuclear magnetic resonance spectroscopy at 7 T. *World J. Radiol.* 3, 105–113. <http://dx.doi.org/10.4329/wjr.v3.i4.105>.
- Sumner, P., Edden, R.A.E., Bompas, A., Evans, C.J., Singh, K.D., 2010. More GABA, less distraction: a neurochemical predictor of motor decision speed. *Nat. Neurosci.* 13, 825–827. <http://dx.doi.org/10.1038/nn.2559>.
- van der Hel, W.S., van Eijsden, P., Bos, I.W.M., de Graaf, R.A., Behar, K.L., van Nieuwenhuizen, O., de Graaf, P.N.E., Braun, K.P.J., 2013. In vivo MRS and histochemistry of status epilepticus-induced hippocampal pathology in a juvenile model of temporal lobe epilepsy. *NMR Biomed.* 26, 132–140. <http://dx.doi.org/10.1002/nbm.2828>.
- van Loon, A.M., Knapen, T., Scholte, H.S., St John-Saaltink, E., Donner, T.H., Lamme, V.A.F., 2013. GABA shapes the dynamics of bistable perception. *Curr. Biol.* 23, 823–827. <http://dx.doi.org/10.1016/j.cub.2013.03.067>.
- Watanabe, M., Maemura, K., Kanbara, K., Tamayama, T., Hayasaki, H., 2002. GABA and GABA receptors in the central nervous system and other organs. *Int. Rev. Cytol.* 213, 1–47.
- Wijtenburg, S.A., Rowland, L.M., Edden, R.A.E., Barker, P.B., 2013. Reproducibility of brain spectroscopy at 7 T using conventional localization and spectral editing techniques. *J. Magn. Reson. Imaging* 38, 460–467. <http://dx.doi.org/10.1002/jmri.23997>.
- Yoon, J.H., Maddock, R.J., Rokem, A., Silver, M.A., Minzenberg, M.J., Ragland, J.D., Carter, C.S., 2010. GABA concentration is reduced in visual cortex in schizophrenia and correlates with orientation-specific surround suppression. *J. Neurosci.* 30, 3777–3781. <http://dx.doi.org/10.1523/JNEUROSCI.6158-09.2010>.
- Zhang, Y., Brady, M., Smith, S., 2001. Segmentation of brain MR images through a hidden Markov random field model and the expectation-maximization algorithm. *IEEE Trans. Med. Imaging* 20, 45–57. <http://dx.doi.org/10.1109/42.906424>.